Silo discharge of binary granular mixtures

M. Madrid,[1] K. Asencio,[2] and D. Maza[2,*]

[1]*Departamento Ingeniería Mecánica, Facultad Regional La Plata, Universidad Tecnológica Nacional, CONICET, Avenida 60 Esquina 124, La Plata 1900, Argentina*

[2]*Departamento de Física y Matemática Aplicada, Facultad de Ciencias, Universidad de Navarra, 31080 Pamplona, Navarra, Spain*

(Received 12 September 2016; published 29 August 2017)

We present numerical and experimental results on the mass flow rate during the discharge of three-dimensional silos filled with a bidisperse mixture of grains of different sizes. We analyzed the influence of the ratio between coarse and fine particles on the profile of volume fraction and velocity across the orifice. By using numerical simulations, we have shown that the velocity profile has the same shape as that in the monodisperse case and is insensitive to the composition of the mixture. On the contrary, the volume fraction profile is strongly affected by the composition of the mixture. Assuming that an effective particle size can be introduced to characterize the mixture, we have shown that previous expression for the mass flow rate of monodisperse particles can be used for binary mixtures. A comparison with Beverloo's correlation is also presented.

DOI: 10.1103/PhysRevE.96.022904

I. INTRODUCTION

The flow of particles through orifices is ubiquitous in industrial processes in which most of the raw or processed materials are stored and delivered in granular form. Despite this fact, there exists no systematic study that links the mass flow rate during silo discharge with the bulk properties of the material delivered, such as the shape of the grains and particle size distribution, or with the silo configuration such as the exit geometry. The most frequently used correlation that links the mass discharged from a silo with the size of its outlet was introduced early in the eighteenth century by Hagen [1,2] and rediscovered during the 1960s by Beverloo *et al.* [3]. The mass flow rate can be written as

$$W = C\rho_B\sqrt{g}[D - kd]^{5/2}, \tag{1}$$

where ρ_B is the bulk density, g is the gravitational acceleration, D is the diameter of the outlet, and d is the diameter of the particle of a monosized granular sample. Values C and k are free parameters introduced *ad hoc* to fit the experimental observations in the range of studied outlet sizes. More than forty years later, Mancok *et al.* [4] provided an expression for the mass flow rate, where the parameter k was excluded and the constant C was replaced by an alternative fitting parameter. Indeed, Mancok *et al.* argued that it is not necessary to introduce k if the dilatancy of the material near the exit is considered. Moreover, these authors fitted an exponential function to the volume fraction at the outlet. However, Mancok's expression—similarly to the Beverloo correlation—was based on an empirical fitting of the experimental results justified only by dimensional arguments. Very recently, the mass flow rate was linked to the microscopic interactions between particles. Janda *et al.* [5] showed that the flow rate of a two-dimensional (2D) silo could be calculated from the particle velocities and volume fraction profiles just at the exit. Both profiles were self-similar and were determined only by the size of the orifice, $D = 2R$. Then, the mass flow rate for a 2D silo can be expressed as

$$W = C\sqrt{g}\phi_\infty[1 - \alpha_1 e^{-R/\alpha_2}]R^{3/2}. \tag{2}$$

In this expression, the constant C is not a free parameter, but a function of the volume fraction and velocity profiles at the outlet and ϕ_∞ is the asymptotic volume fraction at the orifice center in the limit of large apertures. Thus, by analyzing the volume fraction ϕ of the material only at the exit, these authors provided an experimental evidence of the functional form $\phi(x)$ introduced in [5]. Moreover, although α_1 and α_2 in Eq. (2) are in fact fitting parameters, both are linked to the dilatancy of the material near the outlet.

More recently, a 3D silo was studied using numerical simulations to analyze the micromechanical origin of the scaling function introduced in Ref. [5] for the downward velocity profile. Rubio-Largo *et al.* [6] showed that the functional form of the vertical velocity at the outlet is controlled by the kinetic part of a coarse-grained stress tensor, which is indeed controlled by the outlet radius. More importantly, these authors have shown that the vertical velocity profile of the grains at the outlet is nearly insensitive to the diameter of the discharged particle.

The flow of granular mixtures was explored earlier by Artega and Tüzün [7] and Humby *et al.* [8]. In both studies, the authors analyzed the flow rate of a mixture of spherical particles with two different radii and fitted the results with a modified Beverloo correlation. Recently, a similar approach was used by Benyamine *et al.* [9] to study the flow of bidisperse mixtures, but in this case using the mass flow expression Eq. (2) introduced by Janda *et al.* One of the key findings in the work by Benyamine is that the exit velocity of the particles is effectively impacted by the ratio between the particle sizes, and that a typical mixture diameter cannot be simply defined to fit the experimental observations. More recently, Zhou *et al.* [10] provided numerical evidence that the velocity and density profiles of a binary granular mixture at the outlet of a 2D silo have the same functional dependence as the one introduced for the monodisperse case [5]. However, they stated that "the mixture velocity is approximately proportional to the fine mass fractions." Hence, these authors proposed an expression for the

*dmaza@unav.es

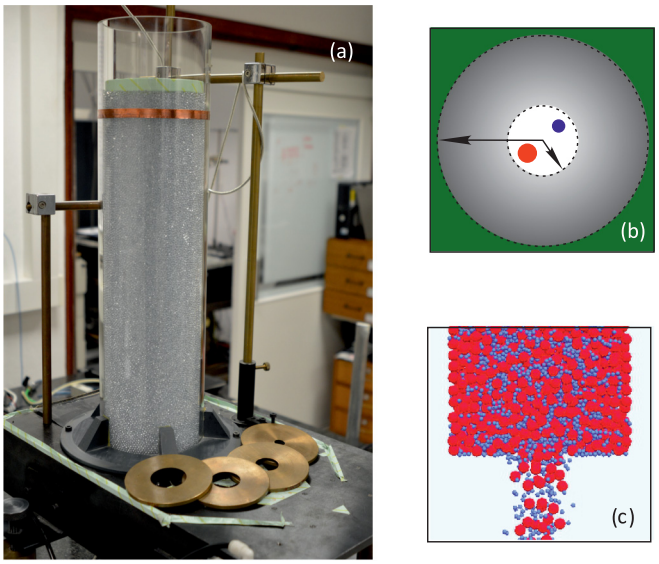

FIG. 1. (a) Photograph of the experimental setup. The interchangeable disks are used to modify the aperture size. (b) Outline of the experimental exit apertures scaled with the particle sizes, $r_c = 0.15$ cm (in red) and $r_f = 0.10$ cm (in blue). The arrows denote the smallest ($R = 0.65$ cm) and largest ($R = 1.95$ cm) studied outlet radius. (c) Snapshot of the simulated case B, in which the particle size ratio was increased to $r_c/r_f = 2.5$.

flow of bidisperse mixtures that includes an alternative fitting constant and a linear combination of two extra functions that depend on the size ratio of the particles with respect to the outlet and on the fine mass ratio.

In this work, we show that a typical mixture particle size can be defined, which agrees with the experimental observations, contrary to the arguments of the work by Benyamine. Furthermore, we show that the scaling approach introduced by Janda *et al.* and Rubio-Largo *et al.* [5,6] can be generalized to the bidisperse case. By the introduction of an effective particle radii the proper scale can be obtained for collapsing all the observational results on a master curve. We show that the downward exit velocity at the outlet is nearly insensitive to the ratio between the mass of fine particles and the total mass, χ_f. Consequently, the differences observed in W for different χ_f are mainly controlled by the volume fraction at the exit. Thereby, the mass flow rate can be calculated as in the monodisperse case if an effective particle radius is used to describe the granular mixture.

II. EXPERIMENTAL AND NUMERICAL PROTOCOLS

A. Experimental setup

All the experiments were done using spherical particles, which pass through an orifice centered in the base of a tall cylindrical silo of a radius of $R_S = 7.50 \pm 0.05$ cm. Glass beads (density: $\rho = 2.40 \pm 0.05$ g/cm^3) with a radius of $r_f = 0.10 \pm 0.05$ cm were used as fine particles and $r_c = 0.15 \pm 0.05$ cm as coarse. The base of the container was exchangeable to carry out experiments with different orifice radii, in the range of 0.65 cm $< R <$ 1.95 cm [see Fig. 1(a)]. A more detailed description of the experimental setup can be found in Mankoc *et al.* [4].

Grains are mixed at different fine mass ratios, $\chi_f = m_f/(m_f + m_c)$ where m_f, m_c are the total mass of the fine and coarse grains, respectively. The beads of each size were poured into the two 1-liter test tubes, the surfaces were leveled with a blade, and the corresponding masses were determined. As we looked for samples where the volume fraction is the same for both monodisperse cases, samples with different masses were rejected, and pouring of both samples was repeated. Afterward, the grains were mixed either before the container was filled, or while the material was fed into the silo. No significant differences in the results have been observed between the two alternative protocols.

In order to determine the discharge rate, two complementary methods were implemented. On the one hand, the mass discharged as a function of time was determined by using a high-capacity, high-resolution electronic balance. On the other hand, the surface downward vertical velocity v_S of the granular column was determined by using an ultrasonic distance meter placed above the silo. During the first half of the discharge duration, the top (free) surface remained almost flat without any signal of a central depression, which indicates the development of a funnel flow regime. Importantly, even in the case where clogging events were observed when small orifices were used, v_S can be measured with good accuracy if the material remains flowing at least for a few seconds.

B. Simulations

To understand the mechanisms behind the observed differences in the mass flow rates when χ_f is varied, a numerical simulation of the discharge process was carried out, using a discrete element method implemented in YADE [11,12]. Then, the velocity and volume fraction profiles at the outlet were carefully determined. Two different cases were considered: case A, which replicated the experimental conditions, and case B, where the density ($\rho = 10$ g/cm^3) of the beads and their sizes ($r_f = 0.5$ cm, $r_c = 1.25$ cm) were increased. Note that in case B $r_c/r_f = 2.5$. These values were selected to enhance any effect that ρ and r_c/r_f could have on the flow properties. Hence, the new size ratio was chosen as a compromise between the aim of enhancing the influence of r_c/r_f and the requirement to avoid segregation during the discharge. Consequently, simulated fine mass ratios of particles for case B were $\chi_f = 0.00$, 0.02, 0.06, 0.16, and 1.00, which correspond to a partial fraction *in number of fine particles*, $N_f/(N_f + N_c)$, of 0, 0.25, 0.50, 0.75, and 1.00, respectively. It is worth noting that for the pure coarse case, the number of particles was $N_c = 2 \times 10^4$, while for the pure fine case the number grew to $N_f = 1.2 \times 10^5$, which represents a notably higher computational cost.

A linear spring–dashpot model was used as the contact force model, with the normal and tangential contact forces expressed as $F_\mathrm{n} = k_\mathrm{n}\xi - \gamma_\mathrm{n}\dot{\xi}$ and $F_\mathrm{t} = \min(\mu F_\mathrm{n}, k_\mathrm{t}\zeta - \gamma_\mathrm{t} v_\mathrm{t})$, respectively. The quantity ξ is the particle-particle overlap, ζ is the total shear displacement of the contact, and v_t is the relative tangential velocity. Furthermore, $k_\mathrm{n} = 2000$ Nm^{-1}, $k_\mathrm{t} = 2k_\mathrm{n}/7$, $\gamma_\mathrm{n} = 0.03$ Nsm^{-1}, $\gamma_\mathrm{t} = 0.02$ Nsm^{-1} and $\mu = 0.55$. The silo was filled to a height of at least four times the

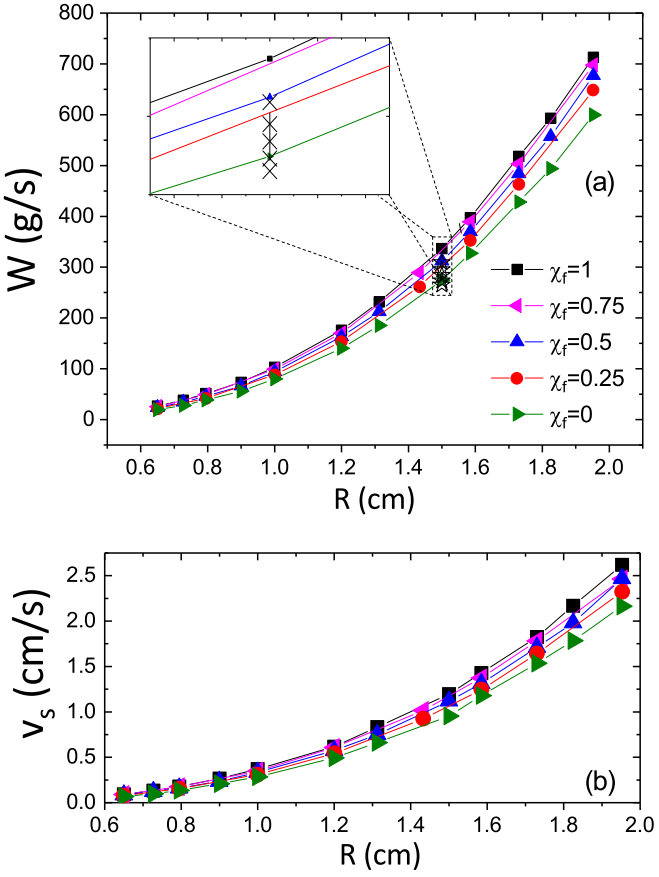

FIG. 2. (a) Experimental mass flow rate W vs the outlet radius R for different fine mass ratios χ_f. The lines are a guide to the eye. Inset: Values obtained from the numerical simulations (case A). The systematic difference between experimental and numerical results is due to the dependence of the bulk density with the filling protocol. (b) Downward free surface velocity as a function of R. In both panels, the standard deviations of the data are smaller than the symbol sizes.

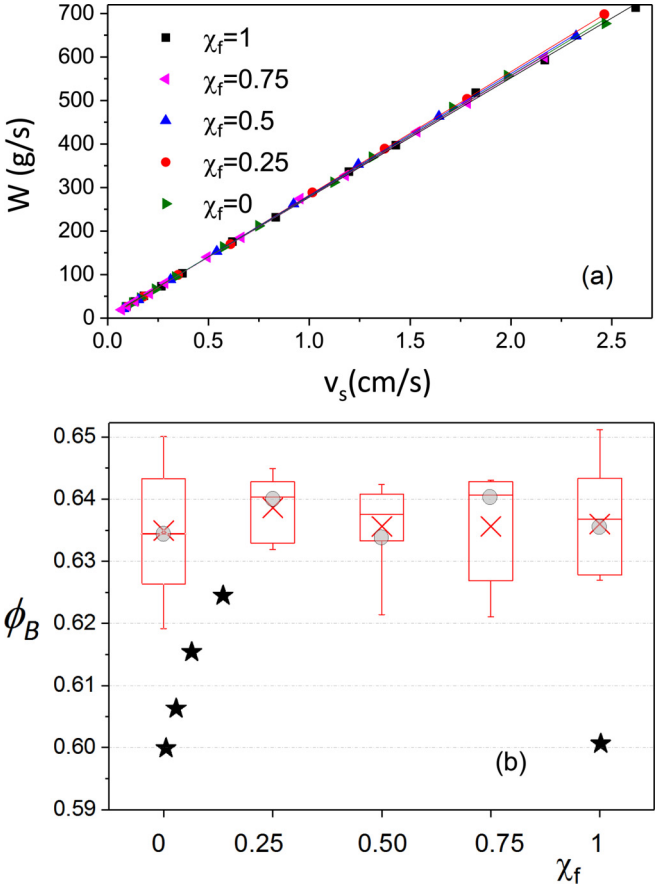

FIG. 3. (a) Experimental mass flow rate against the vertical downward speed of the top free surface. The slopes of different linear fits provide an estimation of the average bulk volume fraction of each mixture [displayed as gray circles in Fig. 3(b)]. (b) Box plot of the experimental bulk volume fraction obtained from all the studied outlet orifices for different values of χ_f. The crosses are the mean values obtained for the different outlet orifices. The up-down boxes correspond to the percentiles 25th and 75th, respectively and the whiskers shows the 10% and 90% limits of the volume fraction distribution. The stars indicate the bulk volume fraction of the simulated case B.

diameter of the silo. Finally, both mixtures flow through a circular orifice of $R = 1.5$ cm and $R = 7.5$ cm for cases A and B, respectively.

III. EXPERIMENTAL AND NUMERICAL RESULTS

A. Experimental results

The mass flow through various orifices was measured for different χ_f. As can be seen in Fig. 2, the larger the fraction of fine particles, the larger the mass flow rate. Indeed, the mass of purely fine particles discharged in 1 s ($\chi_f = 1$), was 20% larger than that of the corresponding $\chi_f = 0$, for the biggest explored outlet ($R = 1.95$ cm). Moreover, the same effect is apparent from the free surface downward velocity, v_S, Fig. 2(b). Figure 3(a) shows that W is linearly correlated with v_S for all the mixtures studied. Therefore, this correlation makes it possible to calculate an average bulk volume fraction for each fine mass ratio. As the bulk volume fraction ϕ_B can be computed for each experimental realization from the simultaneous measures of v_S and W, tens of discharges were measured for each orifice. Then well-defined averages for the bulk volume fraction were obtained for each value of R. These results are summarized using the box plots displayed in Fig. 3(b). In this panel, the bulk density obtained from the linear fit shown in Fig. 3(a) is also included and displayed by gray circles. All these observations confirm that when the coarse-to-fine size ratio is small ($r_c/r_f = 1.5$), results of the bulk volume fraction only slightly affected. However, this almost negligible change in ϕ_B with χ_f has a notable influence on W. To emphasize this observation, we introduce the simulations of case B. In this case, the coarse-to-fine size ratio increases to $r_c/r_f = 2.5$ and the bulk volume fraction changes in a notably larger range [see the star symbols in Fig. 3(b)]. This tendency agrees with the results discussed in Refs. [13] and [14]. Hence, if the coarse-to-fine size ratio has an influence on the flowing properties, it should be apparent from the comparison between cases A and B (see Sec. III B).

Before discussing the microscopic nature of our results, let us analyze the suitability of Beverloo's correlation to predict the mass flow rate of a binary mixture. In Refs. [7,8], the

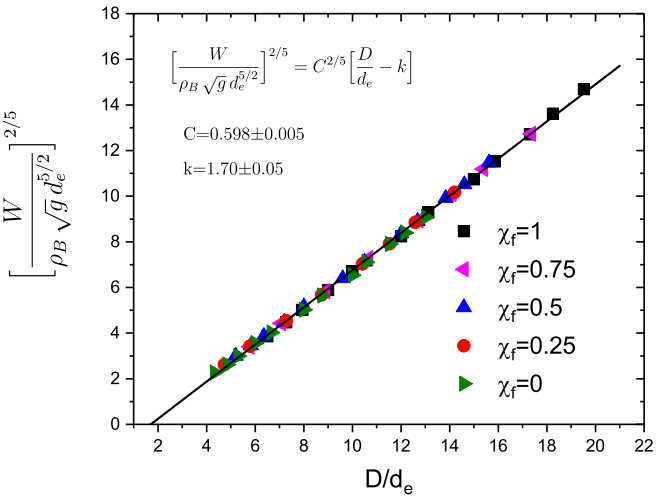

FIG. 4. Dimensionless mass flow rate against the dimensionless outlet size. All experimental data collapse on a single straight line assuming that there exists an effective particle size d_e describing each mixture [see Eq. (4)]. The line corresponds to the fitting the dimensionless Beverloo's expression [Eq. (3)] with the values shown in the legend.

authors chose to fix C to the value introduced by Nedderman [15] and therefore study the influence of χ_f on the fitted value of k. The physical arguments provided to support this criterion are not detailed here. In this case, we fit our results without introducing any restriction to the fitting parameters. Hence, let us write Eq. (1) as

$$W = C\rho_B\sqrt{g}d^{5/2}\left(\frac{D}{d} - k\right)^{5/2}. \tag{3}$$

The right-hand side of Eq. (3) depends on D/d. Thus, to compare the different particles ratios explored, an effective size of the material must be defined. Following the arguments presented by Arteaga *et al.* [7] and Humby *et al.* [8] we used the arithmetic mean size of the beads [16],

$$d_e = 2r_e = 2(\chi_f r_f + (1 - \chi_f)r_c), \tag{4}$$

as the effective diameter to characterize the different granular mixtures. Figure 4 shows the scaled dimensionless mass flow rate as a function of the dimensionless outlet size D/d_e for all the grain mixtures. Clearly, the introduction of d_e allows the experimental results to collapse on a straight line that can be fitted using Eq. (3). Despite the good agreement between the experimental data and Beverloo's expression, there are no mechanical arguments to justify the use of a reduced exit radius $[\frac{D}{d_e} - k]$ in the mass flow rate expression. Moreover, the experimental and numerical evidence suggest that the *empty annulus region*, used to justify the introduction of k, cannot be properly defined [5,6]. In Sec. III C, we use the approach presented in [5] and [6] to avoid the use of the constant k.

B. Numerical results

Velocity and density profiles for different fine mass ratio have been studied using numerical simulations. The vertical velocity $\mathsf{v}(r)$ was calculated at the exit as a function of the

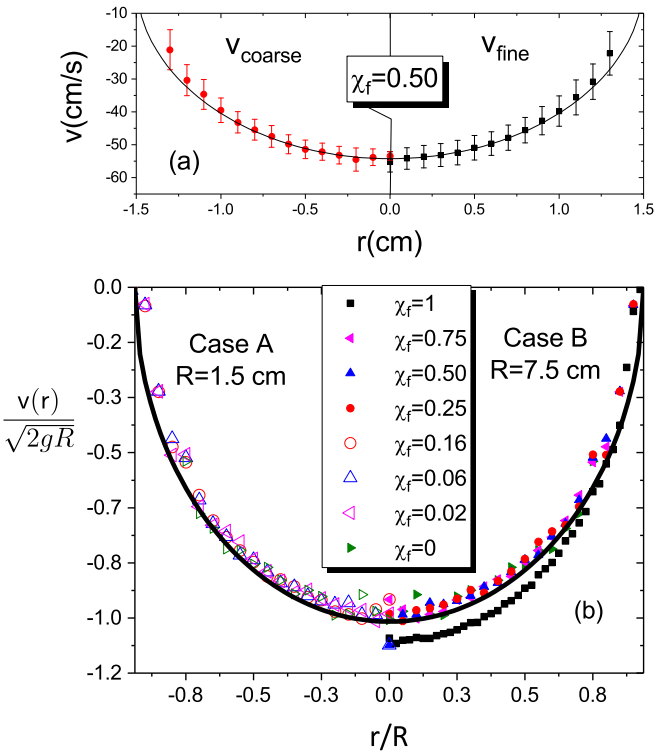

FIG. 5. (a) Profile of the vertical velocity corresponding to the coarse (left panel) and the fine (right panel) particles for case A and $\chi_f = 0.50$. Both profiles are indistinguishable. The solid line corresponds to $\mathsf{v}(r) = \sqrt{2gR}\,[1 - (r/R)^2]^{1/2}$. (b) Velocity profiles corresponding to all χ_f studied were scaled with $\sqrt{2gR}$. The radial coordinate was normalized by the corresponding outlet radius (left panel: case A, $R = 1.5$ cm; right panel: case B, $R = 7.5$ cm). Apart from some minor differences, the exit velocities are marginally affected by the mass or size ratio.

radial coordinate for all particles passing through the orifice. The profiles of the coarse and the fine particles mixed at $\chi_f = 0.50$ are shown in Fig. 5(a) (right and left panels, respectively) for case A. Clearly, both profiles are nearly equivalent. The figure shows that the scaling predicted for monodisperse beads [5], $\mathsf{v}(r) = \sqrt{2gR}\,[1 - (r/R)^2]^{1/2}$, is also valid for each species contained in the mixture [see the continuous line shown in Fig. 5(a)]. Hence, in the following, we use the velocity profile without distinguishing the species.

In order to compare the results corresponding to both simulated conditions (cases A and B), all the velocities were normalized with $\sqrt{2gR}$ (using the corresponding exit radii R). All the profiles are similar to one another, independently of the fine mass ratio. Indeed, all the studied χ_f gives velocities differing by less than 1% from each other, except for $\chi_f = 0$ in case B, which is 7% larger. Consequently, the differences observed in the flow rate (see Fig. 3) cannot be justified by the change in the exit velocities when χ_f was varied.

Figure 6(b) shows that the volume fraction profile at the orifice is very sensitive to χ_f. To check if this dependence could be related to any segregation, we plot the number of fine grains normalized by the total number of particles passing through the concentric circular sections of the orifice [see Fig. 6(a)]. We found that the probability of finding beads of

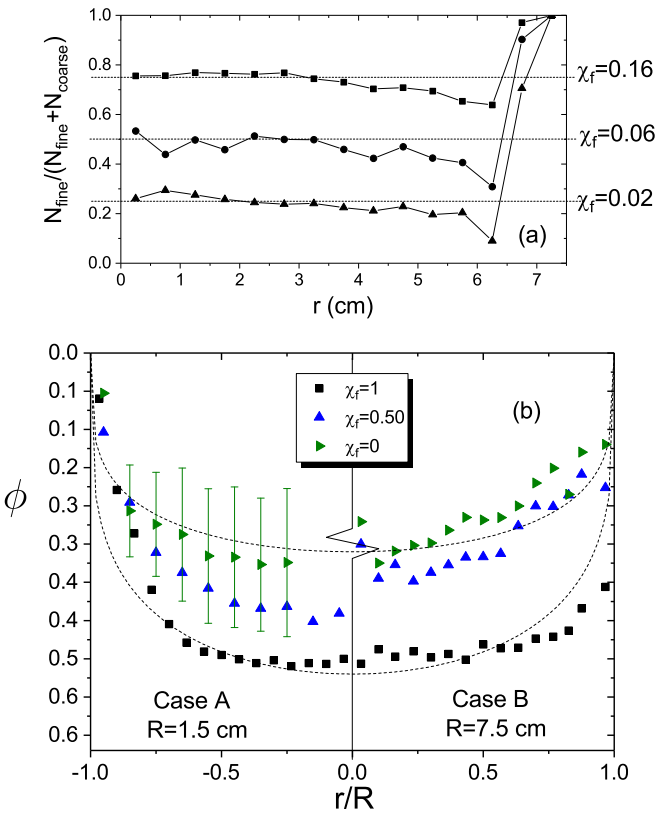

FIG. 6. (a) Normalized number of fine particles passing through a flat annulus of radius r and thickness $\Delta r = r_f$ against r in the simulation (case A). The probability of observing fine particles is almost independent of the radial position and equal to the bulk value (see horizontal lines). (b) Volume fraction of both simulated situations (cases A and B) can be fitted with the same function introduced for the monodisperse limit [5]: $\phi(r) = \phi_c[1-(r/R)^2]^{1/4}$ (shown for the two monodisperse limits by dashed lines). The error bars, corresponding to the standard deviation of the data are similar in all of the cases but they are displayed only for one series of data.

each size in any of these regions is nearly the same as that in the bulk. This fact suggests that the apparent density of the material passing through the outlet could be obtained from the mass weighted arithmetic mean of the mixed particles, as it was done for d_e.

Considering that $\phi(r)$ is compatible with the functional form proposed for the monodisperse case [5], it can be assumed that the radial dependence of the volume fraction can be written as $\phi(r) = \phi_c(R)\,[1-(r/R)^2]^{1/\nu}$. In this expression, $\phi_c(R)$ corresponds to the volume fraction at the center of the orifice of radius R. The different results presented in Fig. 6(b) show that although the shape of the profile is almost not affected by χ_f, the value of ϕ_c depends on χ_f.

C. Mass flow rate estimation

As it was shown in the previous section, the velocity and density profiles at the outlet, $\mathsf{v}(r)$ and $\phi(r)$, can be fitted assuming the same functional dependency, regardless of whether it is a monodisperse material or a granular mixture. Therefore, as in the monodisperse case [5], it is possible to write the expression for the mass flow rate for a given exit radius as

$$W(R) = \iint_{S_o} \rho\phi_c(R)\,\mathsf{v}_c(R)\,[1-(r/R)^2]^{(2+\nu)/2\nu}\,dS_o, \quad (5)$$

where S_o is the outlet surface, ρ is the density of the material, and $\mathsf{v}_c(R)$ is the vertical velocity at the center of the exit. Exponents $1/2$ and $1/\nu$ specify the shape of the velocity and density profiles at the orifice. As $\mathsf{v}(r)$ is independent of χ_f, the velocity at the center of the orifice can be written as $\mathsf{v}_c = \sqrt{2g\gamma R}$, where γ is a correction factor to the vertical acceleration of the particle. This correction has been tested very recently even for a flowing polydisperse system [17]. Then, Eq. (5) can be analytically integrated to obtain

$$W(R) = \rho\,\pi\,\sqrt{g}\,\Omega\,\phi_c(R)\,R^{5/2}, \quad (6)$$

where $\Omega = \frac{\sqrt{2\gamma}}{(\frac{2+\nu}{2\nu}+1)}$ is a dimensionless factor that accounts for the influence of the profiles shape (through the factors 2 and ν) and the vertical acceleration (through the factor γ) on the flow expression. Furthermore, $\phi_c(R)$ is *a priori* an unknown function but its functional dependence can be determined only by plotting $\Omega\,\phi_c(R) = \frac{W(R)R^{2/5}}{\rho\pi\sqrt{g}}$ against R as shown in Fig. 7(a). Clearly, an exponential saturation can fit any of the data sets. More importantly, the value of $\Omega\phi_c$ is almost independent of χ_f for $R \to \infty$.

Figure 7(b) shows all the experimental results introduced as a function of the reduced orifice radius $R' = R/r_e$ [$r_e = d_e/2$; see Eq. (4)]. All the scaled data collapse on a single curve. Therefore, the fit of the collapsed data [Fig. 7(b)] suggests that an effective scale α could be used to characterize the shape of the packing fraction profile at the outlet:

$$\Omega\phi_c(R') = \phi_\infty[1-e^{-R'/\alpha}]. \quad (7)$$

Here, ϕ_∞ is the asymptotic value of $\Omega\phi_c$ when the size of the outlet tends to infinity, and α is the typical scale over which the exit orifice has a significant influence. The value of α is around ten times the effective size [see the inset of Fig. 7(b)] of the granular material r_e.

Equation (6) can be rewritten for any granular media defined by an effective radius of r_e in a more compact form as

$$W(R/r_e) = C'\,[1-e^{-(R/r_e)/\alpha}]\left[\frac{R}{r_e}\right]^{5/2}, \quad (8)$$

where $C' = \rho\,\pi\sqrt{g}\,\phi_\infty\,r_e^{5/2}$ is the scale imposed by the radial dependence of the velocity and volume fraction profiles and the effective particle size.

Figure 8 shows that all results (numerical and experimental) are in good agreement with Eq. (8) independently of χ_f. The continuous line represents Eq. (8) using the value of C' calculated from the fitting parameters $\phi_\infty = 0.638$ and $\alpha = 8.524$ and the effective radius r_e corresponding to each fine mass ratio χ_f studied. The dashed line represents Berverloo's correlation using the values introduced in Fig. 4 as fitting parameters. The small difference between both fits becomes more noticeable in the log-log plot of the same data (inset of Fig. 8).

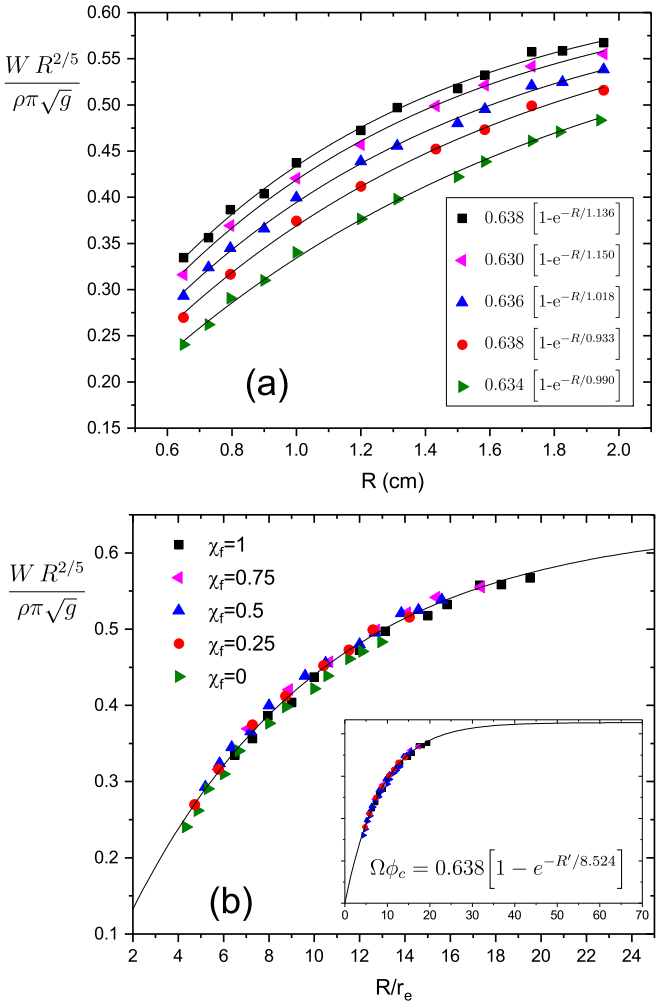

FIG. 7. (a) Dimensionless mass flow rate against the outlet radius R. Each set of data has been fitted using the exponential saturation indicated on the label. (b) All data can be collapsed in a single curve when plotted against the normalized radius, $R' = \frac{R}{r_e}$. The inset shows the values used to fit the collapsed results.

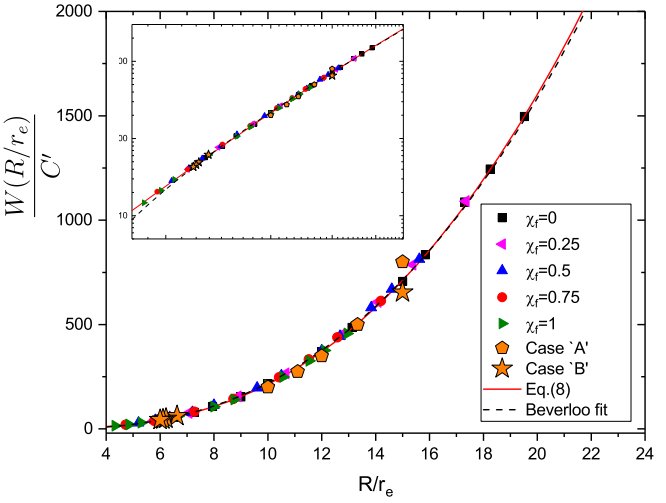

FIG. 8. Collapsed data corresponding to the simulated and experimental mass flow rates. For the sake of convenience, values of W and R have been normalized by the radius r_e to compare all the results. The continuous line corresponds to Eq. (8) with the parameter C' calculated using $\phi_\infty = 0.638$ and $\alpha = 8.524$ and the corresponding effective radius of r_e. The dashed line represents Berverloo's correlation using the parameters introduced in Fig. 4. Inset: log-log plot of the same data where the small difference between both fitting protocols becomes noticeable.

IV. CONCLUSIONS

We have numerically and experimentally studied the mass discharge process of a flat-bottom silo filled with a binary mixture of spherical beads. In order to enhance the possible effects that the coarse-to-fine size ratio could have on the discharge dynamics, we performed numerical simulations of heavier particles with a coarse-to-fine size ratio not accessible to our experimental setup. The numerical results confirm that (a) no significant segregation take place during the discharge and (b) the inertia of the beads and their sizes seem to have no major influence on the exit velocity of the particles.

Using the mass-weighted arithmetic mean radius as the effective particle size for the binary mixture, we showed that the velocity and the volume fraction profiles at the outlet can be fitted by the scaling relationship, discussed by Janda *et al.* and Rubio-Largo *et al.* [5,6]. Moreover, we found that while the velocity profile does not depend on the fine mass ratio, the volume fraction is affected by χ_f.

Motivated by these findings, we analyzed the experimental results considering the approaches by Beverloo and Janda to predict the silo mass flow rate. Both procedures provide good predictions (Fig. 8). Nevertheless, Eq. (8) connects the discharge rate with the dynamics observed at the outlet, while the approach by Beverloo uses two free parameters to fit the results. The analysis of the grain dynamics summarized by Eq. (7) indicates that a pertinent "granular scale" governs the observed dynamics. This scale is controlled by the microscopic interaction between particles through the frictional forces and the restitution coefficient. Hence, the presented results indicate that, while no segregation occur, the mass flow rate for a binary mixture of grains could be formally predicted with the continuous approach introduced for the monodisperse case [5], if a suitable effective size for the granular mixture is defined.

ACKNOWLEDGMENTS

This work was partially funded by the Ministerio de Economía y Competitividad (Spanish Government) through Grants No. FIS2011-26675 and No. FIS2014-57325 and by ANPCyT (Argentina) through Grant No. PICT-2012-2155. We are especially indebted to R. C. Hidalgo and L. A. Pugnaloni for their useful comments and criticism. K.A. thanks Asociación de Amigos de la Universidad de Navarra for the scholarship.

[1] G. Hagen, Akadamie der Wissencschaften zu Berlin, 35 (1852).
[2] B. P. Tighe and M. Sperl, Granular Matter **9**, 141 (2007).
[3] W. Beverloo, H. Leniger, and V. de Velde, Chem. Eng. Sci. **15**, 260 (1961).

[4] C. Mankoc, A. Janda, R. Arévalo, J. M. Pastor, I. Zuriguel, A. Garcimartín, and D. Maza, Graular Matter **9**, 407 (2007).
[5] A. Janda, I. Zuriguel, and D. Maza, Phys. Rev. Lett. **108**, 248001 (2012).
[6] S. M. Rubio-Largo, A. Janda, D. Maza, I. Zuriguel, and R. Hidalgo, Phys. Rev. Lett. **114**, 238002 (2015).
[7] P. Arteaga and U. Tüzün, Chem. Eng. Sci. **45**, 205 (1990).
[8] S. Humby, U. Tüzün, and A. Yu, Chem. Eng. Sci. **53**, 483 (1998).
[9] M. Benyamine, M. Djermane, B. Dalloz-Dubrujeaud, and P. Aussillous, Phys. Rev. E **90**, 032201 (2014).
[10] Y. Zhou, P. Ruyer, and P. Aussillous, Phys. Rev. E **92**, 062204 (2015).
[11] V. Smilauer, E. Catalano, B. Chareyre, S. Dorofeenko, J. Duriez, N. Dyck, J. Elias, B. Er, A. Eulitz, A. Gladky, N. Guo, C. Jakob, F. Kneib, J. Kozicki, D. Marzougui, R. Maurin, C. Modenese, L. Scholtes, L. Sibille, J. Stransky, T. Sweijen, K. Thoeni, and C. Yuan, *Yade Documentation*, 2nd ed. (Zenodo, 2015).
[12] L. Pournin, T. M. Liebling, and A. Mocellin, Phys. Rev. E **65**, 011302 (2001).
[13] I. Biazzo, F. Caltagirone, G. Parisi, and F. Zamponi, Phys. Rev. Lett. **102**, 195701 (2009).
[14] M. Clusel, E. I. Corwin, A. O. N. Siemensa, and J. Brujic, Nature (London) **460**, 611 (2009).
[15] R. M. Nedderman, *Statistics and Kinematics of Granular Materials*, 1st ed. (Cambridge University Press, Cambridge, 1992).
[16] M. Alderliesten, J. Biopharm. Stat. **15**, 295 (2005).
[17] S. M. Rubio-Largo, D. Maza, and R. C. Hidalgo, Comp. Part. Mech. (2016), doi: 10.1007/s40571-016-0133-4.